U.S. National Library of Medicine
National Center for Biotechnology Information

NLM Citation: Chopra A. ^{64}Cu-Labeled PEGylated nano-graphene oxide (GO) covalently linked to NOTA-conjugated anti-CD105 (endoglin) chimeric monoclonal antibody TRC105. 2012 May 17 [Updated 2012 Jun 28]. In: Molecular Imaging and Contrast Agent Database (MICAD) [Internet]. Bethesda (MD): National Center for Biotechnology Information (US); 2004-2013.
Bookshelf URL: https://www.ncbi.nlm.nih.gov/books/

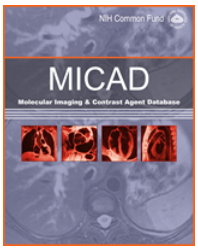

^{64}Cu-Labeled PEGylated nano-graphene oxide (GO) covalently linked to NOTA-conjugated anti-CD105 (endoglin) chimeric monoclonal antibody TRC105

[^{64}Cu]-NOTA-GO-TRC105

Arvind Chopra, PhD[1]

Created: May 17, 2012; Updated: June 28, 2012.

Chemical name:	^{64}Cu-Labeled PEGylated nano-graphene oxide (GO) covalently linked to NOTA-conjugated anti-CD105 (endoglin) chimeric monoclonal antibody TRC105	
Abbreviated name:	[^{64}Cu]-NOTA-GO-TRC105	
Synonym:		
Agent Category:	Antibody	
Target:	CD105 (endoglin) antigen	
Target Category:	Antigen	
Method of detection:	Positron emission tomography (PET)	
Source of signal / contrast:	^{64}Cu	
Activation:	No	
Studies:	• *In vitro* • Rodents	Structure not available in PubChem.

Background

[PubMed]

The CD105 antigen (endoglin) is a hypoxia-inducible, 180-kDa, disulfide-linked, homodimeric transmembrane glycoprotein that is a co-receptor for the transforming growth factor β (TGF-β) (1). Both CD105 and TGF-β are expressed at low levels in resting endothelial cells, but they are overexpressed in cancerous lesions and play a significantly proangiogenic role in remodeling the vasculature of malignant tumors (2). It has been shown that the levels of CD105 in endothelial tissues correlate well with the degree of cell proliferation and that the antigen is a suitable biomarker to quantify tumor angiogenesis and can be used to determine the prognostic outcome for cancer patients (3). The biological activity of CD105 has been discussed in detail by Seon et al. (4). Investigators have demonstrated that immunotoxins and radioimmunoconjugates generated with anti-CD105 monoclonal antibodies (mAbs) can inhibit angiogenesis and prevent the growth and metastasis of cancerous tumors (4). For

Author Affiliation: 1 National Center for Biotechnology Information, NLM, Bethesda, MD 20894; Email: micad@ncbi.nlm.nih.gov.

translation to the clinic, a human/mouse chimeric anti-CD105 mAb (designated c-SNj6 or TRC105) was generated, and shown to have suitable pharmacokinetic, toxicological, and immunogenicity characteristics for use in non-human primates (5). Currently, a clinical trial is in progress to evaluate the use of TRC105 for the treatment of metastatic breast cancer.

TRC105 has been labeled with ^{64}Cu (6) and ^{89}Zr (7), respectively, and has been reported to detect the expression of CD105 with positron emission tomography (PET) imaging in xenograft tumors in mice. In another study, TRC105 was conjugated to IRDye 800CW, a near-infrared fluorescent (NIRF) dye, and the expression of CD105 in tumors was visualized with NIRF imaging (8). TRC105 has also been conjugated with ^{64}Cu and IRDye 800CW to develop a dual-modality (PET/NIRF) imaging agent that can be used to detect murine breast cancer 4T1 cell tumors in mice (9). Recently, TRC105 was conjugated to 1,4,7-triazacyclononane-1,4,7-triacetic acid (NOTA) and labeled with ^{66}Ga, and the radioimmunoconjugate was shown to be suitable for the visualization of CD105 expression with PET in 4T1 cell xenograft tumors in mice (10).

Investigators have recently become interested in the use of PEGylated graphene oxide (GO; to read about the physical and chemical properties of graphene, see Feng and Liu (11)), a carbon-based material, in biomedical applications such as drug delivery (12), cancer therapy (13), and preclinical *in vivo* imaging and ablation of tumors in mice (14). In a proof-of-principle study, Hong et al. (15) used PET to evaluate ^{66}Ga-labeled NOTA covalently linked to a sheet of PEGylated nano-GO conjugated to TRC105 (NOTA-GO-TRC105) for the biodistribution and visualization of xenograft tumors that express the CD105 antigen in mice. In a similar study with a different tumor model the biodistribution and efficacy of ^{64}Cu-labeled NOTA-GO-TRC105 ([^{64}Cu]-NOTA-GO-TRC105) to detect xenograft tumors that expressed the CD105 in mice was investigated with PET (16).

Related Resource Links

TRC105 chapters in MICAD

Other anti-CD105 antibody chapters in MICAD

Human CD105 (endoglin) protein and mRNA sequences

CD105 gene information (Gene ID: 2022)

CD105 in Online Mendelian Inheritance in Man Database (OMIM)

Clinical trials related to TRC105

Synthesis

[PubMed]

The covalent linking of NOTA to PEGylated GO (NOTA-GO) and the synthesis of NOTA-GO-TRC105 for radiolabeling with ^{64}Cu for *in vivo* PET imaging and biodistribution studies is described elsewhere (16). Fluorescein isothiocyanate (FITC)-labeled GO (FITC-GO) and FITC-GO-TRC105 were synthesized to investigate the *in vitro* binding affinity and specificity of the complexes for CD105 with fluorescence techniques (16). The average number of NOTA molecules covalently linked to a sheet of GO was not reported. The average small sheet size range of NOTA-GO and NOTA-GO-TRC105 was 10–50 nm as determined with atomic force microscopy (16). The average diameters of the two GO conjugates were 21.9 ± 0.6 nm and 27.0 ± 0.9 nm, respectively, as determined with dynamic light scattering measurements (16). The zeta-potentials of NOTA-GO and NOTA-GO-TRC105 were determined to be −9.46 ± 4.74 mV and 0.08 ± 5.35 mV, respectively (16).

NOTA-GO and NOTA-GO-TRC105 were respectively labeled with ^{64}Cu, and the radiolabeled products were purified on PD-10 columns with phosphate-buffered saline (pH not reported) as the mobile phase (16). The preparation and purification procedures for [^{64}Cu]-NOTA-GO or [^{64}Cu]-NOTA-GO-TRC105 were completed in 90 ± 10 min (n = 10 preparations). The radiochemical yields, radiochemical purities, and specific activities of both [^{64}Cu]-NOTA-GO and [^{64}Cu]-NOTA-GO-TRC105 were reported to be 76 ± 8% (based on 30 μg NOTA-GO or NOTA-GO-TRC105), >95%, and ~0.9 GBq/mg (24.3 mCi/mg), respectively.

In Vitro Studies: Testing in Cells and Tissues

[PubMed]

The stability of [^{64}Cu]-NOTA-GO and [^{64}Cu]-NOTA-GO-TRC105 was investigated by incubating the respective tracers in complete mouse serum at 37°C for up to 48 h, and the incubation mixtures were sampled at various time points to determine the percentage of radioactivity retained on the GO conjugates (16). Both ^{64}Cu-labeled GO conjugates were reported to retain >90% of the radioactivity at all the time points as determined with filtration through a 100-kDa cutoff filtration device. This study indicated that the two radiolabeled complexes would have excellent stability under *in vivo* conditions.

Flow cytometric analysis of HUVEC cells (human umbilical vein endothelial cells that have a high expression of CD105) exposed to 50 μg/mL FITC-GO-TRC105 (based on GO content) showed that the cells had >570-fold higher fluorescence intensity compared with the untreated cells (16). Treatment of HUVEC cells with FITC-GO or TRC105 alone enhanced the fluorescence only by ~6-fold. Cells blocked with 3.33 nmol TRC105 and then treated with FITC-GO-TRC105 as above had ~100-fold lower fluorescence intensity compared with cells exposed to FITC-GO-TRC105 alone. This indicated that FITC-GO-TRC105 bound specifically to the CD105 antigen on the surface of the HUVEC cells. Minimal fluorescence was observed in MCF-7 cells (a human breast cancer epithelial cell line that does not express the CD105; used as a negative control in this study), indicating that FITC-GO-TRC105 exhibited low non-specific binding to the cells.

Animal Studies

Rodents

[PubMed]

The biodistribution of [^{64}Cu]-NOTA-GO and [^{64}Cu]-NOTA-GO-TRC105 was investigated in mice bearing murine breast cancer 4T1 cell tumors as described by Hong at al (16). The animals (n = 4 mice/group) were injected with the tracer (5–10 MBq (135–270 μCi) in each mouse) through the tail vein and euthanized at 3 h and 48 h postinjection (p.i.). All the major organs, including the tumors, were retrieved from the animals to determine the amount of radioactivity accumulated in the various tissues. Data obtained from the study were presented as percent of injected dose per gram tissue (% ID/g). With both radiolabeled GO conjugates, the label was detected at 3 h p.i. mainly in the liver (~17.5% ID/g), followed by blood (~10.0% ID/g and ~15% ID/g for [^{64}Cu]-NOTA-GO-TRC105 and [^{64}Cu]-NOTA-GO, respectively), and spleen (~10% ID/g for both [^{64}Cu]-NOTA-GO-TRC105 and [^{64}Cu]-NOTA-GO). Tumors of mice injected with [^{64}Cu]-NOTA-GO-TRC105 showed a significantly higher uptake of label (~6.0% ID/g; $P < 0.05$) compared with the amount detected in the lesions of mice injected with [^{64}Cu]-NOTA-GO (~2.0% ID/g). All other organs showed a radioactivity uptake of <2.5% ID/g with both the tracers at all the time points. By 48 h p.i., the uptake of radioactivity from both tracers was similar in the blood (~2.5% ID/g), liver (~12.5% ID/g), spleen (~10% ID/g), and the tumors (~2.5% ID/g). Another group of mice (n = 4 animals) given a blocking dose of NOTA-GO-TRC105 (33.33 nmol/kg body weight) 2 h before administration of the radiolabeled GO immunoconjugate were euthanized at 48 h p.i. The accumulation of radioactivity in the blood, liver, spleen, and tumors of these animals was comparable to the uptake observed at 48 h p.i. in the normal tissues and lesions of animals injected with [^{64}Cu]-NOTA-GO-

TRC105 alone (16). The insignificant difference in the uptake of radioactivity between the tumors of the "blocked" animals and the lesions of animals injected with [^{64}Cu]-NOTA-GO-TRC105 alone was attributed to clearance of the label from the tissues due to metabolism and degradation of the conjugate (16).

For PET imaging of mice bearing 4T1 cell tumors (n = 4 animals), the rodents were injected with 5–10 MBq (135–270 μCi) [^{64}Cu]-NOTA-GO-TRC105 or [^{64}Cu]-NOTA-GO through the tail vein, and static whole-body images of the animals were acquired at 0.5 h, 3 h, 16 h, 24 h, and 48 h p.i (16). Quantitative data for the various organs and the tumors were obtained from the images with region-of-interest analysis as described by Hong et al. (16). The amount of tracer in the blood was 9.7 ± 1.3% ID/g, 6.6 ± 0.5% ID/g, 4.4 ± 0.5% ID/g, 4.3 ± 0.2% ID/g, and 3.9 ± 0.1% ID/g at 0.5, 3, 16, 24, and 48 h p.i., respectively, and the amount of label in the liver was 18.6 ± 1.3% ID/g, 14.1 ± 2.1% ID/g, 12.4 ± 1.9% ID/g, 13.2 ± 1.2% ID/g, and 13.7 ± 1.3% ID/g at 0.5, 3, 16, 24, and 48 h p.i., respectively. The tumors were clearly visible at 0.5 h p.i. and showed a relatively stable uptake of radioactivity at all the time points (5.8 ± 0.6% ID/g, 5.3 ± 0.6% ID/g, 4.5 ± 0.6% ID/g, 4.0 ± 0.4% ID/g, and 3.4 ± 0.1% ID/g at 0.5, 3, 16, 24, and 48 h p.i., respectively). At all the time points, the accumulation of radioactivity from [^{64}Cu]-NOTA-GO-TRC105 in the muscles was reported to be <0.5% ID/g. In general, with [^{64}Cu]-NOTA-GO the level and pattern of radioactivity uptake in the liver and blood was similar to that observed with [^{64}Cu]-NOTA-GO-TRC105. With [^{64}Cu]-NOTA-GO, the accumulation of the tracer in the tumors was 2.0 ± 0.3% ID/g, 2.1 ± 0.4% ID/g, 1.9 ± 0.4% ID/g, 2.2 ± 0.4% ID/g, and 2.4 ± 0.3% ID/g at 0.5, 3, 16, 24, and 48 h p.i., respectively, but the uptake in the lesions was significantly lower than that observed with [^{64}Cu]-NOTA-GO-TRC105 ($P < 0.05$) at all these time points.

To determine the *in vivo* target-binding specificity of [^{64}Cu]-NOTA-GO-TRC105, the animals (n = 4 mice) were injected with 13.3 nmol nonradioactive TRC105 2 h before administration of the ^{64}Cu-labeled GO immunoconjugate (16). PET images of the animals were acquired as before. The uptake of label in the tumors was calculated to be 2.0 ± 0.5% ID/g, 2.1 ± 0.3% ID/g, 2.6 ± 0.4% ID/g, 2.7 ± 0.3% ID/g, and 2.8 ± 0.2% ID/g at 0.5, 3, 16, 24, and 48 h p.i., respectively, which was significantly lower ($P < 0.05$ at all the time points) than the accumulation observed in the lesions of animals injected with [^{64}Cu]-NOTA-GO-TRC105 alone (for uptake values, see above). The amount of radioactivity detected in the liver and blood of animals given the blocking dose was similar to that of animals injected with [^{64}Cu]-NOTA-GO-TRC105 alone at all the time points (the amount of radioactivity in the liver was 15.3 ± 2.0% ID/g, 14.6 ± 2.1% ID/g, 12.5 ± 1.7% ID/g, 11.9 ± 1.3% ID/g, and 11.4 ± 1.3% ID/g at 0.5, 3, 16, 24, and 48 h p.i., respectively, and in the blood it was 10.2 ± 1.3% ID/g, 6.9 ± 0.9% ID/g, 5.3 ± 0.5% ID/g, 4.8 ± 0.2% ID/g, and 2.9 ± 0.1% ID/g at 0.5, 3, 16, 24, and 48 h p.i., respectively). Therefore, this study confirmed the *in vivo* binding specificity of the GO-radioimmunoconjugate to the CD105 antigen (16).

To confirm the uptake of NOTA-GO-TRC105 in CD105-specific tissues of mice bearing 4T1 cell tumors, the animals (n = 3 mice) were injected with 5 mg/kg body weight of the non-radiolabeled GO-immunoconjugate and euthanized at 3 h p.i (16). The tumors, liver, spleen, and muscles of the rodents were harvested, frozen, and cryo-sectioned for histological examination. Light microscopy revealed that high levels of NOTA-GO-TRC105 were present (seen as dark spots) only in tissue sections of the tumors, liver, and spleen, but not in the muscles of these animals. However, NOTA-GO was observed only in the sections of liver and spleen tissues obtained from animals injected with this GO-chelating agent complex. This study demonstrated that NOTA-GO-TRC105 specifically targets the CD105 antigen in the tumor. Immunofluorescence staining of the tissue slices for CD31 (a biomarker for the vasculature), with anti-mouse CD31 as the primary antibody and for CD105 using the TRC105 within NOTA-GO-TRC105 as the primary antibody, showed that the uptake of NOTA-GO-TRC105 in the liver and spleen was due to the non-specific capture of the complex by the reticuloendothelial system and not due to the specific targeting of CD105 on the vasculature. Almost no uptake of NOTA-GO-TRC105 was observed in the muscles and other normal tissues of the animals (16).

From these studies, the investigators concluded that [^{64}Cu]-NOTA-TRC105 is a suitable agent to detect tumors that express the CD105 antigen in rodents (15).

Other Non-Primate Mammals

[PubMed]

No publication is currently available.

Non-Human Primates

[PubMed]

No publication is currently available.

Human Studies

[PubMed]

No publication is currently available.

Supplemental Information

[Disclaimers]

No information is currently available.

NIH Support

This work was supported in part by a grant from the National Institutes of Health through the UW Radiological Sciences Training Program 5 T32 CA009206-32.

References

1. Nassiri F., Cusimano M.D., Scheithauer B.W., Rotondo F., Fazio A., Yousef G.M., Syro L.V., Kovacs K., Lloyd R.V. *Endoglin (CD105): a review of its role in angiogenesis and tumor diagnosis, progression and therapy.* . Anticancer Res. 2011;31(6):2283–90. PubMed PMID: 21737653.
2. Perez-Gomez E., Del Castillo G., Juan Francisco S., Lopez-Novoa J.M., Bernabeu C., Quintanilla M. *The role of the TGF-beta coreceptor endoglin in cancer.* . ScientificWorldJournal. 2010;10:2367–84. PubMed PMID: 21170488.
3. Fonsatti E., Nicolay H.J., Altomonte M., Covre A., Maio M. *Targeting cancer vasculature via endoglin/CD105: a novel antibody-based diagnostic and therapeutic strategy in solid tumours.* . Cardiovasc Res. 2010;86(1):12–9. PubMed PMID: 19812043.
4. Seon B.K., Haba A., Matsuno F., Takahashi N., Tsujie M., She X., Harada N., Uneda S., Tsujie T., Toi H., Tsai H., Haruta Y. *Endoglin-targeted cancer therapy.* . Curr Drug Deliv. 2011;8(1):135–43. PubMed PMID: 21034418.
5. Shiozaki K., Harada N., Greco W.R., Haba A., Uneda S., Tsai H., Seon B.K. *Antiangiogenic chimeric anti-endoglin (CD105) antibody: pharmacokinetics and immunogenicity in nonhuman primates and effects of doxorubicin.* . Cancer Immunol Immunother. 2006;55(2):140–50. PubMed PMID: 15856228.
6. Hong H., Yang Y., Zhang Y., Engle J.W., Barnhart T.E., Nickles R.J., Leigh B.R., Cai W. *Positron emission tomography imaging of CD105 expression during tumor angiogenesis.* . Eur J Nucl Med Mol Imaging. 2011;38(7):1335–43. PubMed PMID: 21373764.

7. Hong H., Severin G.W., Yang Y., Engle J.W., Zhang Y., Barnhart T.E., Liu G., Leigh B.R., Nickles R.J., Cai W. *Positron emission tomography imaging of CD105 expression with 89Zr-Df-TRC105.* . Eur J Nucl Med Mol Imaging. 2012;39(1):138–48. PubMed PMID: 21909753.
8. Yang Y., Zhang Y., Hong H., Liu G., Leigh B.R., Cai W. *In vivo near-infrared fluorescence imaging of CD105 expression during tumor angiogenesis.* . Eur J Nucl Med Mol Imaging. 2011;38(11):2066–76. PubMed PMID: 21814852.
9. Zhang Y., Hong H., Engle J.W., Yang Y., Theuer C.P., Barnhart T.E., Cai W. *Positron Emission Tomography and Optical Imaging of Tumor CD105 Expression with a Dual-Labeled Monoclonal Antibody.* . Mol Pharm. 2012;9(3):645–53. PubMed PMID: 22292418.
10. Engle J.W., Hong H., Zhang Y., Valdovinos H.F., Myklejord D.V., Barnhart T.E., Theuer C.P., Nickles R.J., Cai W. *Positron emission tomography imaging of tumor angiogenesis with a (66)ga-labeled monoclonal antibody.* . Mol Pharm. 2012;9(5):1441–8. PubMed PMID: 22519890.
11. Feng L., Liu Z. *Graphene in biomedicine: opportunities and challenges.* . Nanomedicine (Lond). 2011;6(2):317–24. PubMed PMID: 21385134.
12. Yang K., Wan J., Zhang S., Zhang Y., Lee S.T., Liu Z. *In vivo pharmacokinetics, long-term biodistribution, and toxicology of PEGylated graphene in mice.* . ACS Nano. 2011;5(1):516–22. PubMed PMID: 21162527.
13. Yang K., Zhang S., Zhang G., Sun X., Lee S.T., Liu Z. *Graphene in mice: ultrahigh in vivo tumor uptake and efficient photothermal therapy.* . Nano Lett. 2010;10(9):3318–23. PubMed PMID: 20684528.
14. Zhang W., Guo Z., Huang D., Liu Z., Guo X., Zhong H. *Synergistic effect of chemo-photothermal therapy using PEGylated graphene oxide.* . Biomaterials. 2011;32(33):8555–61. PubMed PMID: 21839507.
15. Hong H., Zhang Y., Engle J.W., Nayak T.R., Theuer C.P., Nickles R.J., Barnhart T.E., Cai W. *In vivo targeting and positron emission tomography imaging of tumor vasculature with (66)Ga-labeled nano-graphene.* . Biomaterials. 2012;33(16):4147–56. PubMed PMID: 22386918.
16. Hong H., Yang K., Zhang Y., Engle J.W., Feng L., Yang Y., Nayak T.R., Goel S., Bean J., Theuer C.P., Barnhart T.E., Liu Z., Cai W. *In vivo targeting and imaging of tumor vasculature with radiolabeled, antibody-conjugated nanographene.* . ACS Nano. 2012;6(3):2361–70. PubMed PMID: 22339280.